



City Research Online

City St George's, University of London

Citation: Khader, M. A., Ghavami, M., Al-Zaili, J. & Sayma, A. I. (2024). Residential Micro-CHP system with integrated Phase change material thermal energy storage. *Energy*, 300, 131606. doi: 10.1016/j.energy.2024.131606

This is the published version of the paper.

This version of the publication may differ from the final published version. To cite this item please consult the publisher's version.

Permanent repository link: <https://openaccess.city.ac.uk/id/eprint/32892/>

Link to published version: <https://doi.org/10.1016/j.energy.2024.131606>

Copyright and Reuse: Copyright and Moral Rights remain with the author(s) and/or copyright holders. Copies of full items can be used for personal research or study, educational, or not-for-profit purposes without prior permission or charge, unless otherwise indicated, provided that the authors, title and full bibliographic details are credited, a hyperlink and/or URL is given for the original metadata page and the content is not changed in any way. For full details of reuse please refer to [City Research Online policy](#).



Residential Micro-CHP system with integrated phase change material thermal energy storage

Mahmoud A. Khader^{a,*}, Mohsen Ghavami^b, Jafar Al-Zaili^b, Abdalnaser I. Sayma^b

^a Department of Mechanical Engineering, School of Physics, Engineering and Computer Science, University of Hertfordshire, College Lane Campus, Hatfield, AL10 9AB, UK

^b Department of Engineering, City, University of London, Northampton Square, London, EC1V 0HB, UK

ARTICLE INFO

Keywords:

Combined heat and power
Thermal energy storage
Phase change material
Heat Exchanger

ABSTRACT

This paper presents an analysis and experimental investigation of the effect of integrating Phase Change Material (PCM) within a heat exchanger within a Micro Combined Heat and Power (Micro-CHP) system intended for residential applications. A commonly used Micro-CHP layout is replicated in a test rig to characterise the performance of two alternative heat exchanger arrangements. The first is a conventional arrangement where the exhaust gas produced by the prime mover is directed to an air-to-water heat exchanger to heat water and store it in a tank. In the second arrangement, PCM material is encapsulated within specially designed compartments in a heat exchanger to store part of the exhaust thermal energy from the prime mover while heating the water in the storage tank. The time needed to heat the water and discharge heat is compared for both cases, as well as the amount of thermal energy stored during the same operating period. The study also explored the potential to improve the designed unit by using different PCM materials. The test results show that adding 4.7 L capacity paraffin compartments within the heat exchanger extended the discharge time of the hot water by over 400 %, which reflects a marked improvement in the heat storage capacity of the system. This would result in a significant increase in the viable operating period of a CHP system. The one-dimensional analysis revealed that replacing the paraffin with ClimSel C58 PCM can reduce the charging time of the water tank by around 54 % improve the heat storage capacity by factor of 2.35 comparing to Paraffin. The proposed heat exchanger with encapsulated PCM has a potential in other applications such as storage of excess renewable energy or integration with heat pumps to improve matching of supply and demand and thus flexibility of an energy system with integrated intermittent renewables.

1. Introduction

CHP technology, particularly those using renewable fuels, could form an important part of an integrated decarbonised energy system supporting the drive towards net-zero targets. By utilising the low-grade heat from a thermal power cycle, CHP technologies can achieve thermal efficiency approaching 90 % [1,2]. Micro-CHP refers to systems with an electricity generation capacity of less than kW, mainly used in domestic applications as a replacement for fossil fuel-fired boilers [3]. Various micro-CHP technologies have been deployed such as those based on micro-gas turbines, internal combustion reciprocating engines, Sterling engines and fuel cells. The main function of the micro-CHP systems for residential applications is to generate heat, while the excess electricity

generated can be fed to the grid. The usual ratio of heat to electricity generation in a micro-CHP system is about 6:1 [4].

In the UK, the number of installed CHP plants has increased in the last two decades. Meanwhile, unstable prices of electricity and gas, the lack of heat distribution networks and insufficient governmental incentives form an obstacle that hinders the expansion of CHP installations [5,6]. Hence, further innovations and development of CHP systems could support overcoming some of these issues through providing low carbon, low running cost and secure energy supply systems. This research is focused on improving the heat storage capacity of micro-CHP systems by adding PCM compartments to the exhaust heat exchanger. This significantly improves the heat storage capacity of the system, reduces the size of the required water storage tank, and reduces the operating time of the prime mover to provide the heating needs for a

* Corresponding author.

E-mail addresses: m.khader@herts.ac.uk (M.A. Khader), m.ghavami@city.ac.uk (M. Ghavami), Jafar.Alzaili@city.ac.uk (J. Al-Zaili), a.sayma@city.ac.uk (A.I. Sayma).

<https://doi.org/10.1016/j.energy.2024.131606>

Received 11 October 2023; Received in revised form 16 April 2024; Accepted 9 May 2024

Available online 12 May 2024

0360-5442/© 2024 The Authors. Published by Elsevier Ltd. This is an open access article under the CC BY license (<http://creativecommons.org/licenses/by/4.0/>).

Nomenclature		air	air
Letters		in	Inlet
h	Average heat transfer coefficient (W/m ² .K)	out	Outlet
k	Thermal conductivity (W/m.K)	t	Total
Q	Heat transfer rate	1–6	Referring to points T1-T6 in Fig. 7
\dot{m}	Mass flow rate	Abbreviations	
C_p	Constant pressure heat capacity	CHP	Combined Heat and Power
ρ	Density	DAQ	Data Acquisition
T	Temperature (K)	HE	Heat Exchanger
R	Thermal Resistance	NI	National Instruments
h	Convective heat transfer coefficient	PCM	Phase Change Material
Greeks		RTD	Resistance Thermometer
μ	Dynamic viscosity (m ² /s)	SCADA	Supervisory Control and Data Acquisitions
\varnothing	The polar angle between the riblets cusp and the rotor axis	TES	Thermal Energy Storage
Subscripts		TESHE	Thermal Energy Storage Heat Exchanger

particular application.

For CHP systems to replace the boiler at residential premises, they should adapt to effectively meet the fluctuating demand for hot water. CHP units without thermal storage cannot respond quickly to changes in heat demand, therefore, a thermal storage unit is typically added to the system to improve its flexibility and to cope with the variation in heat load [7–9].

The techno-economic assessment of the advantages of integrating TES with CHP plants has been studied by a number of researchers. Lepiksaar et al. [10] investigated analytically the effect of coupling a CHP plant with Thermal Energy Storage (TES) tanks of different capacities ranging from 3000 to 150,000 m³. The study compared the different arrangements in terms of gas consumption and heat rejection reduction. The ability to store the excess heat during low heat demand periods and to utilise this heat when the demand is high or when the electricity price is high provides extra operational flexibility to the CHP plant. The results of this study show that natural gas consumption can be reduced by 19 % and heat rejection by 26 % when the CHP plant is coupled with a 150,000 m³ thermal storage tank.

Volkova et al. [11,12] assessed the economic and environmental benefits of TES with a CHP-based district heating plant. The thermal power rating of the CHP plant in the study was 76 MW_{thermal} and the storage tank capacity varied from 1000 to 30,000 m³. The results revealed that the TES integration has a positive effect on the economic indicators of the plant (net present value and internal return rate). On the environmental side, using a TES of water tank capacity of 30,000 m³ leads to 30,000 tonnes of CO₂ savings in two weeks of operation.

Verda et al. [13] evaluated the cost reduction and energy saving that can be achieved by integrating TES with a CHP plant used for district heating. They found that integrating TES results in a reduction of the total operating hours of the system and energy consumption of the Plant dropped by 12 %, and the reduction in the total operational and capital costs can reach up to 5 %.

Fragaki et al. [14] studied the economics of a CHP plant operating with a gas engine and thermal storage based on British market conditions. They identified the most economically feasible size for a plant used for district heating of a thermal load of 20,000 MWh per year is a 3 MWe gas engine with a 215 m³ thermal storage vessel. The economic analysis of the optimum plant configuration reflects that the integration of TES can double the return on investments compared with the same CHP plant without TES.

The studies on the viability of thermal storage were not limited to large CHP plants. Many researchers investigated the benefit of using thermal storage in micro-CHP systems. Johara et al. [15] experimentally studied the effectiveness of a micro-CHP system that uses an Erythritol-filled shell and tube heat exchanger as a thermal storage

reservoir. The addition of thermal storage reduced the specific fuel consumption which resulted in a drop in the CO₂ and NO_x emissions.

To estimate the effect of adding TES on the sizing and performance of micro-CHP systems, Pérez-Iribarren et al. [16] studied a number of arrangements for micro-CHP systems (including CHP without TES configuration) to determine the layout with the highest performance. The study showed that connecting the TES directly to the CHP and the utility equipment which allows simultaneous charging and discharging of the unit results in the highest thermodynamic performance and the largest economic revenue.

The operating temperature for the residential hot water utilities lies between 65 and 85 °C which makes water the best candidate for a heat storage media as it can be directly connected to those utilities without the need to have an extra heat exchanger added to the CHP system. Moreover, water is nontoxic, cheap and has a relatively high specific heat capacity. All of those made water the most used thermal storage material in residential CHP units [17].

Phase change materials have recently gained popularity amongst researchers as a potential thermal storage media. These materials utilise the latent heat stored during the transition from one phase to another which enables a greater amount of heat to be stored or ejected per unit volume [18]. This high energy density of the PCM materials leads to reducing the overall weight and size of the CHP units, which results in saving space in the residential premises. This could be of particular importance in crowded urban locations where space availability is limited, and space cost is high. In comparison with water, PCMs such as paraffin wax PHC6568 can store the same amount of energy by occupying around 31 % less volume, while PCM salt such as H105 can store the same amount of energy by occupying around 64 % less volume [19]. Several researchers have explored the effect of adding PCM to solar water storage tanks on the energy density and discharge time. Fazilati et al. [20] were able to achieve a 25 % elongation of the energy discharge time by adding Paraffin wax capsules to the water storage tank with a volume fraction ratio of 55 % (Paraffin/water). In a different study, Cabeza et al. [21] achieved a 16.4 % increase in energy density by adding a granular graphite compound to a water tank with a volume fraction ratio of 4.1 % (PCM/Water).

Previous studies have focused on investigating the feasibility of integrating thermal storage with CHP systems and the impact of adding PCM to water storage tanks. The present work studies experimentally and analytically the behaviour of a new design for a heat exchanger with embedded PCM compartments intended for integration with a CHP system for residential building heating applications. The proposed design aims to enhance the Micro-CHP systems' operational flexibility and thermal storage capacity, reducing the system size and cost and extending the CHP prime mover's life.

2. Methodology

As pointed out earlier, this study aims at characterising a new design for a heat exchanger with embedded PCM for Micro-CHP systems. Hence, the storage unit was built and tested under operating conditions similar to those found in domestic Micro-CHP systems. The test results then were analysed and verified using a non-dimensional model for heat transfer in the heat exchanger compartments.

Section 3 discusses the design of the thermal storage and PCM material selection. Section 4 explains the layout of test rig, operating conditions and the measurement system used in the experiments.

3. Thermal storage unit

Micro-CHP systems for residential and small businesses are designed to be as compact as possible, ideally to occupy the same volume as conventional boilers. This was the motivation to investigate new designs of thermal storage units. With the current development of additive manufacturing techniques, it was possible to design a Thermal Storage integrated into a Heat Exchanger (TESHE). In this case, the need for a separate thermal storage unit is eliminated which reduces the size and, potentially, the cost of the whole system. Fig. 1 shows the designed prototype, where the exhaust air passes through the vertically aligned channels. They are bounded by the water chambers from one side and the PCM chambers on the other side. In this prototype unit, 18 thermocouples are placed at different heights to measure the temperature of the PCM at various locations to have a better understanding of the thermal unit behaviour by mapping the temperature distribution within the PCM material. The water in this unit flows in the vertical slots as well, and it flows in the same direction as the air. This specific design of the unit aimed at maximising the size of the PCM chambers. The material of TESHE was chosen to be Inconel 718 as it doesn't react with the chosen PCM material. The structural dimensions of the TESHE unit are listed in Table 1.

3.1. PCM material selection

The selection of a suitable Phase change materials (PCMs) is crucial in the design of TESHE for heating applications as they are restricted to certain temperature range and storage capacity [22]. As the largest portion of heat storage happens during the melting of the PCM, thus the melting point of the selected PCM must be close to the target operating temperature of the working fluid used in the heating system, which is water in residential heating systems. Heating systems are normally operated at water temperature between 80 and 60 °C [23], consequently

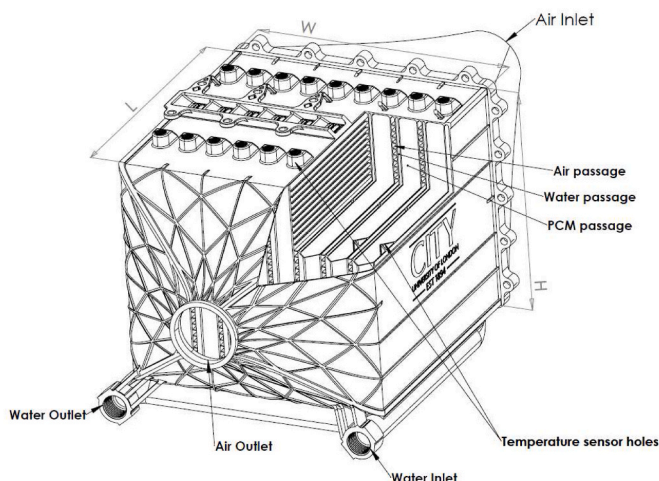


Fig. 1. City University of London's thermal storage unit.

Table 1

Structural details of the TESHE unit.

Component	Dimension
Unit Dimensions (excluding inlet and discharge converging and diverging diffusers)	L x W x H (200 x 210 x 180) [mm]
Water compartment volume	0.65 [litre]
Water passage width	2 mm
Air passage width	3.5 mm
PCM passage width	15 mm
PCM compartment volume	4.7 [litre]
Air inlet/discharge pipe diameter	2 [inch]

the PCM must have a melting point in the same range. Compatibility is another important aspect when selecting the PCM, where chemical reactions need to be avoided between the PCM and the encapsulation material [24]. For this purpose, Paraffin wax (PHC6568) has been selected to serve as a storage media. This material is commercially available, low price compared to other PCM materials, has stable thermophysical properties, disposable and non-toxic which make it easy to handle during preparation for testing [25]. Paraffin PHC6568 melting range is 64–66 °C and its latent heat storage capacity is 187354 J/kg. Table 2 presents the thermophysical properties of this material [26].

4. Test rig

A test rig has been developed to experimentally characterise the behaviour of the TESHE at different operating conditions. Fig. 2 shows a schematic drawing for the test rig setup. The test rig was built to mimic the same setup for a CHP system integrated with a heating water circuit. The hot exhaust gas stream was replaced by a stream of air supplied by the workshop air supply. Supply air is then heated to the desired temperature via a 40 kWe electric heater before entering the TESHE. The water circuit is represented by a storage tank and a pump to circulate the water in the TESHE. A view of the test rig is shown in Fig. 3.

To perform this test, cold air supply is driven through the heater to increase its temperature and is then blown down the TESHE. At the same time the water pump starts circulating the water in the water circuit. The Supervisory Control and Data Acquisitions (SCADA) system based on Lab-VIEW software and National Instruments™ hardware were used in the test rig. The output power of the heater and the air flow regulator valve were controlled using the voltage and current signals generators in the SCADA system, which provides control over the temperature and the flow rate of the air stream entering the TESHE. Whilst the pump was operated at constant flow rate mode to reduce the number of variables in the test procedure.

The test procedure comprises of two phases that are the charging and discharging of the water tank. In the charging phase, the water tank is being heated from the room temperature to reach around 70°C (store thermal energy). During the charging process the cold supply air is heated by passing through the heater coils and blew down the heat exchanger while the water circuit is running. In the discharge process, the energy stored in the water tank is removed by cutting off the power supply of the heater and allowing the cold air to pass through the TESHE till the water tank temperature drops below 40 °C.

Table 2

Paraffin wax PHC6568 properties [26].

Material	Property
Melting range	64–66 °C
Latent heat capacity	187 kJ/kg
Viscosity @ 100 °C	5.0–7.0 cSt
Density solid	829 kg/m ³
Density liquid	789 kg/m ³

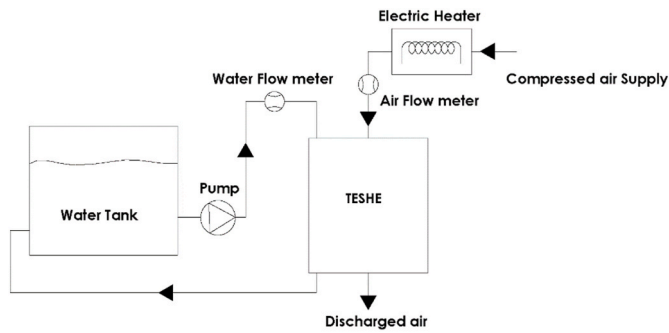


Fig. 2. Schematic for the test rig layout.



Fig. 3. TESHE test rig.

4.1. Measurements

As stated earlier, this experiment aims to characterise the TESHE unit and examine the feasibility of integrating a thermal storage material into the heat exchanger used in CHP systems. This requires measuring the temperature of the air and water streams at the inlet and discharge of the TESHE and the temperature of the PCM during the charging and discharging phases. Furthermore, the mass flow rates of the air and water streams and the pressure drop across the unit are required.

For this purpose, 18 k-type thermocouples were inserted at various depths in the PCM chambers (see Fig. 1). This type of thermocouples is not the highest accuracy among the common thermocouples, but it has a high temperature range which allows testing the unit using higher melting temperature PCMs. The temperature of air at the inlet and discharge of the TESHE was measured using another k-type thermocouple, while the water stream at the inlet and discharge of the unit were measured via resistance thermometers RTD PT100 which offer better accuracy. The thermocouples and the RTDs signals were logged to a computer through a National Instruments (NI) 9213 and 9217 Data Acquisition (DAQ) modules respectively. These modules have a high accuracy in reading the temperature (± 0.02 °C) when operating at room temperature (23 °C). All the thermocouples were calibrated using a dry block calibrator. The calibration data were implemented in the software and the final reading was displayed to monitor the measurements during the test.

During the test, the operating air pressure was measured at three stations: after the flow meter and at the TESHE inlet and discharge ports. The first one is required to calculate the mass flow rate of air and the other two are for determining the flow condition and calculating the pressure drop in the unit. After the flow meter, the static pressure was

measured using 3 mm tube attached to the wall of the pipe. At the inlet and discharge ports of the TESHE, the total pressure was measured using a total pressure probe aligned with the pipe centre line. For both measurements, current output gauge pressure transducer with operating range from 0 to 2 bars absolute were used. The outputs of all the transducers were logged to the computer through NI 9203 DAQ. This module has eight channels to read 4–20 mA signals with accuracy of ± 0.02 mA when operates at the room temperature. The vortex flow meter Rosemount 8800d was used to measure the air flow rate. The output signal of this device is 4–20 mA, and its accuracy is $\pm 9.5e-4$ m³/s.

5. Results and discussion

As mentioned earlier, the main purpose of this study is to investigate the effect of adding thermal storage capability to a heat exchanger used in a micro-CHP unit. For this purpose, the storage unit was initially tested as a Heat Exchanger HE (air-water) without adding the PCM and then it was tested as TESHE (air-water-PCM). The test operating conditions are listed in Table 3. Different performance parameters were monitored in the test including the air pressure drop in the unit, heat transfer rate, and charging and discharging times.

Fig. 4 shows the inlet air and the water tank temperatures during the charging phase for both cases (HE and TESHE). The results show that the production of hot water is not affected by adding the PCM into the heat exchanger. That is, the time need to raise the water temperature in the tank to a certain level is the same in both cases. Once the TESHE is designed to utilise the exhaust air from a power generation, the results confirm that the power generation unit doesn't require to operate for extended time period to charge the hot water tank.

Fig. 5 shows the inlet air and the water tank temperatures during the discharge phase for both units. The discharge process started by cutting off the power supply of the heater and allowing the cold air to pass through the TESHE till the water tank temperature drops below 40 °C. In the case of HE, the discharge time was 266 s, while in the case of TESHE the unit discharged in 1431 s this represents 438 % increase in the discharging time without affecting the charging time. This result can be seen in Fig. 6, where the heat transfer rate from the air during charging process is greater in the case of TESHE, which allows storing a larger amount of energy without affecting the water tank charging time. The heat transfer rate in Fig. 6 was calculated using equation (1).

$$Q_{air} = \dot{m}_{air} C_{p-air} (T_{air-in} - T_{air-out}) \quad (1)$$

Where Q_{air} is the heat transfer rate from the air stream [Watt], \dot{m}_{air} is the air mass flow rate [kg/s], C_{p-air} is the air specific heat capacity [J/kg.K] and $T_{air-out}$, T_{air-in} are the air temperature at the discharge and inlet of the HE respectively [k].

To investigate this further, a steady state one-dimensional resistance model of the unit was developed. Fig. 7 shows a cross-sectional view of the heat exchanger compartments, where the exhaust Air passage is bounded by the PCM compartment from the right and with the water passage from the left. The following assumptions were made.

- 1 The aspect ratio (height of the passage to its thickness) is large enough to assume one dimensional heat transfer in the lateral direction of the unit.

Table 3
Test operating conditions.

Variable	Property
Test cell temperature	22 °C
Water flow rate	6 liters/s
Air Flow rate	215 g/s

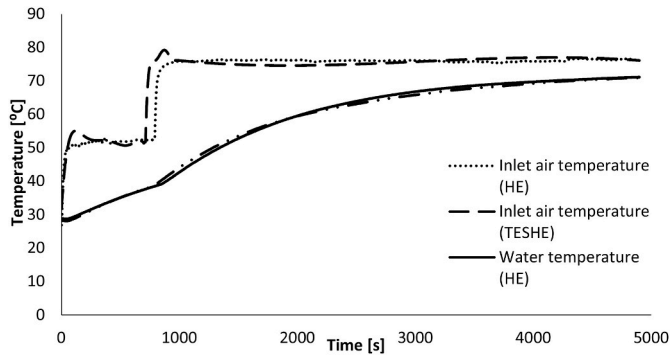


Fig. 4. water tank and inlet air temperatures during charging phase for HE and TESHE.

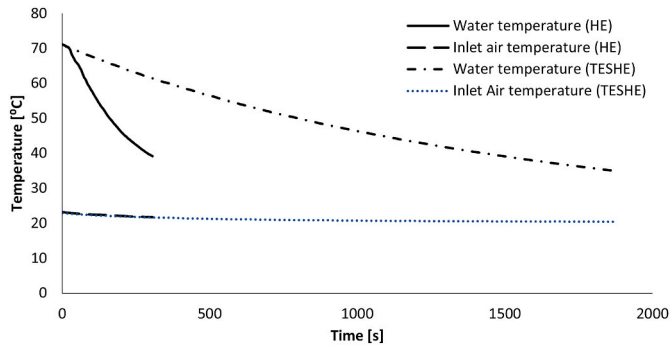


Fig. 5. water tank and inlet air temperatures during discharge phase for HE and TESHE.

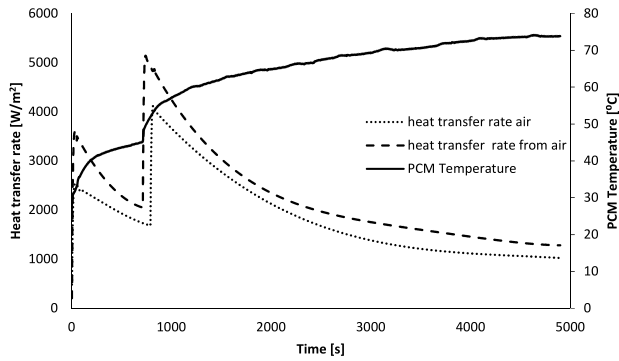


Fig. 6. Heat transfer rate from air stream.

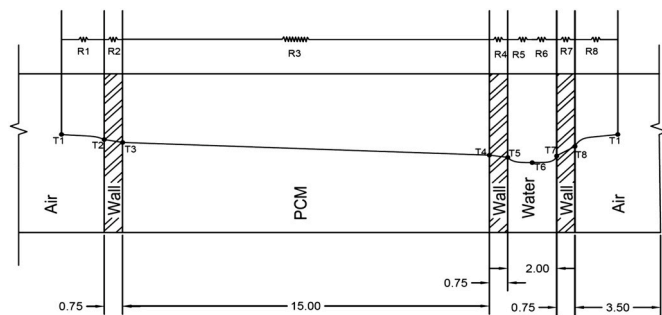


Fig. 7. thermal resistance model for the heat exchanger unit.

- 2 The materials used (Inconel, paraffin, water, and air) have homogeneous properties.
- 3 The effect of radiation has been neglected because of the small temperature difference and low temperature values.

For a steady-state, one-dimensional heat transfer from air to water through metal wall, PCM slab and wall in series, the rate of heat (Q) transferred due temperature gradient is the same across each section.

$$Q_{1-2(conv)} = Q_{2-3(cond)} = Q_{3-4(cond)} = Q_{4-5(cond)} = Q_{5-6(conv)} \quad (2)$$

Where station 1–6 are referring to points T1–T6 in Fig. 7. In this case, the total thermal resistance (R_{t_TESHE}) between point 1 and point 6 is given as:

$$R_{t_TESHE} = R_1 + R_2 + R_3 + R_4 + R_5 \quad (3)$$

$$R_1 = \frac{1}{h_1} \quad (4)$$

$$R_2 = R_4 = \frac{l_w}{k_w} \quad (5)$$

$$R_3 = \frac{l_{PCM}}{k_{PCM}} \quad (6)$$

$$R_5 = \frac{1}{h_6} \quad (7)$$

Where h_1 and h_6 are the convection heat transfer coefficient at the air and water sides respectively. l_w is the metal wall thickness and l_{PCM} is the PCM slab thickness. k_w and k_{PCM} are the thermal conductivity of metal and PCM, respectively.

In the case of HE with no PCM, air replaces the PCM slab, and the heat is mainly transferred via convection. Thus, the total thermal resistance can be calculated using equation (8). Table 4 lists the values of k and h used to calculate the total resistance.

$$R_{t_HE} = \frac{1}{h_1} + \frac{l_w}{k_w} + \frac{1}{h_3} + \frac{l_w}{k_w} + \frac{1}{h_6} \quad (8)$$

For heat transfer from the air to water through the metal wall (left side of air passage, refer to Fig. 7), the thermal resistance is not affected too by adding the PCM, thus it was not considered in the comparison.

In the case of TESHE the total thermal resistance was calculated to be 0.042 [$m^2.K/W$], and in the case of HE it was 0.1473 [$m^2.K/W$]. This reduction in the thermal resistance explains why the water tank charging time wasn't affected even though part of the air thermal energy was used to raise the PCM temperature.

To examine the accuracy of the one-dimensional model, the heat transfer rate was calculated using the model and compared with the experimental data. The resulting values are plotted in Fig. 8, where it can be seen that the 1-D model results are very close to the experimental results.

It can also be noticed that once the temperature difference diminishes the heat transfer rate approaches zero in the case of the 1-D model whilst the experimental calculations doesn't. This result is expected as the 1-D model uses the temperature difference between the air and water (T_1 , T_6 , refer to Fig. 7) to calculate the heat transfer rate but in the experimental case, the air inlet and discharge temperatures were

Table 4
Test operating conditions.

Variable	Property
h_1 (air side)	300 [$W/m^2.K$]
h_6 (water side)	950 [$W/m^2.K$]
h_3	7 [$W/m^2.K$]
k_w (Inconel 718)	15 [$W/m.K$]
k_{PCM} [solid]	0.2 [$W/m.K$]

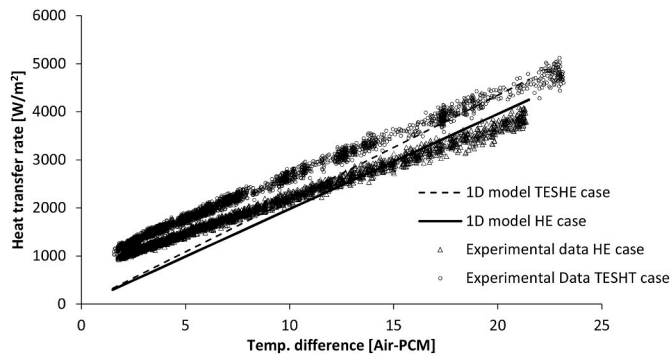


Fig. 8. Heat transfer rate from the exhaust air stream.

used (refer to equation (1)). This also can explain the higher heat transfer rate resulting from the experimental measurements, where the heat transfer gained from the inlet and discharge temperature includes the heat losses to the ambient as the TESHE unit wasn't insulated during the test.

To extend this study further, the 1D model was used to study the effect of using different PCM material suitable for the same application. Table 5 lists the material considered for the study and their properties.

Starting with the charging time, Fig. 9 shows effect of changing the PCM on the total thermal resistance between the hot airstream and the water for each material (refer to equation (3)). It is evident that using varying the PCM material can reduce the charging time by reducing the thermal resistance between air and water streams, thus using PulseICE-S70 can reduce the resistance by 58 % compared to Paraffin wax. Similarly replacing Paraffin with ClimSel C58 results in 54 % reduction in thermal resistance. Another important aspect to study, is the thermal energy storage capacity of the unit using different PCMs. Fig. 10 shows that Paraffin has the lowest storage capacity amongst all the PCMs under consideration, whilst ClimSel C58 has the highest capacity. Considering both factors, thermal resistance of the unit and its capacity, it is clear that using ClimSel C58 can reduce the charging time of the water tank and ramp up the heat storage capacity by factor of 2.35 compared to the tested unit.

6. Conclusion

In this paper, a heat exchanger with embedded PCM compartments was tested experimentally to study its thermal characteristics and its capability to improve CHP systems' performance. From this study, the following conclusions can be drawn.

- Adding PCM to the heat exchanger resulted in improving the thermal storage capacity of the system, which reflected on extending the discharge time for the unit from 266 [s] to 1432 [s] which is 438 % increase in the discharge time.
- With the improvement in thermal storage, adding the TESHE reduces the size of the water storage tank of the CHP unit compared to same unit with conventional HE, which will result in cost and size reduction of the system.

Table 5
PCM materials' properties.

PCM material	Melting Temp, C	Latent Heat, kJ/kg	Thermal Conductivity, W/m.K	Density, kg/m3	Volumetric Heat capacity (MJ/m3)
Paraffin wax -PHC6568	64–66	187	0.2	829	155
ClimSel C58 [27]	55–58	260	0.5	1400	364
Rubitherm -RT70HC [28]	69–71	260	0.2	880	229
Rubitherm -RT90HC [29]	90–91	170	0.2	950	162
PulseICE-S70 [30]	70	100	0.57	1680	168
PulseICE-X70 [30]	70	160	0.36	1085	174

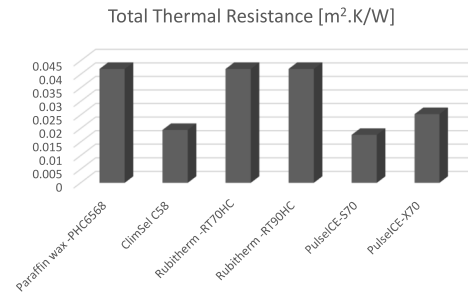


Fig. 9. Total thermal resistance ($R_{t-TESHE}$) between point 1 and point 6 within the thermal storage for different PMC material.

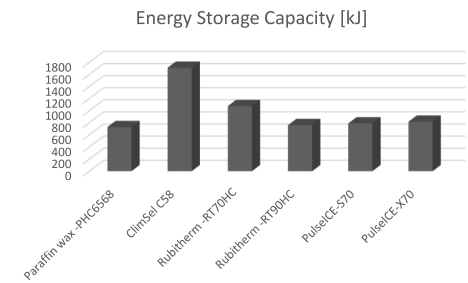


Fig. 10. Total thermal energy storage capacity for the TESHE.

- Paraffin wax was use as a PCM for its safety, availability and price compared to other PCM candidates, but the one-dimensional analysis revealed that replacing the paraffin with ClimSel C58 can reduce the charging time of the water tank and ramp up the heat storage capacity by factor of 2.35 comparing to Paraffin.
- The current design of the TESHE wasn't optimised to either reduce the pressure drop nor to maximise the heat transfer between the exhaust air stream and both water and PCM. In the coming studies, the design will be studied numerically to identify possible improvements to the design which would pave the way to optimise the HE geometry and to maximise its performance, reduce its size and reduce pressure losses.

CRediT authorship contribution statement

Mahmoud A. Khader: Writing – review & editing, Writing – original draft, Validation, Supervision, Software, Methodology, Investigation, Formal analysis, Data curation, Conceptualization. **Mohsen Ghavami:** Writing – review & editing, Validation, Investigation, Data curation. **Jafar Al-Zaili:** Writing – review & editing, Validation, Investigation. **Abdulnaser I. Sayma:** Writing – review & editing, Supervision, Funding acquisition.

Declaration of competing interest

The authors declare that they have no known competing financial

interests or personal relationships that could have appeared to influence the work reported in this paper.

Data availability

The experimental data used in the research is included within the paper

References

- [1] Sycom O. Review of combined heat and power technologies. Office OF energy efficiency and renewable energy. USA: U.S. DEPARTMENT OF ENERGY; 1999.
- [2] Jimenez-Navarro JP, Kavvadias K, Filippidou F, Pavičević M, Quoilin S. Coupling the heating and power sectors: the role of centralised combined heat and power plants and district heat in a European decarbonised power system. *Applied Energy* 2020;270:115134.
- [3] E. & I. S. U. Department for Business. Combined heat and power technologies -A detailed guide for CHP developers – Part 2. London: OGL; 2021.
- [4] Energy Saving Trust, Micro combined heat and power, 05 08 2022. [Online]. Available: <https://energysavingtrust.org.uk/advice/micro-combined-heat-and-power/>. [Accessed 8 February 2023].
- [5] E. & I. S. U. Department for Business. Policy paper: British energy security strategy [Online]. Available: <https://www.gov.uk/government/publications/british-energy-security-strategy/british-energy-security-strategy>; April 2022.
- [6] Simader G, Krawinkler R, Trnka T. Micro CHP systems: state-of-the-art. Vienna: Austrian Energy Agency; 2006.
- [7] Salman CA, Li H, Li P, Yan J. Improve the flexibility provided by combined heat and power plants (CHPs) –a review of potential technologies. *e-Prime - Advances in Electrical Engineering, Electronics and Energy* 2021;1:15.
- [8] Li P-W, Chan Cl. Thermal energy storage analyses and designs. Elsevier Inc.; 2017.
- [9] Hast A, Rinne S, Syri S, Ki J. The role of heat storages in facilitating the adaptation of district heating systems to large amount of variable renewable electricity. *Energy* 2017;137:775–88.
- [10] Lepiksaar K, Masatin V, Latosov E, Siirde A, Volkova A. Improving CHP flexibility by integrating thermal energy storage and power-to-heat technologies into the energy system. *Smart Energy* 2021;2:100022.
- [11] Volkova A, Latosov E, Siirde A. Heat storage combined with biomass CHP under the national support policy. A case study of Estonia. *Environmental and Climate Technologies* 2020;24(1):171–84.
- [12] Volkova A, Latošov E, Andrijaškin M, Siirde A. Feasibility of thermal energy storage integration into biomass CHP-based district heating system. *CHEMICAL ENGINEERING TRANSACTIONS* 2018;70. <https://doi.org/10.3303/CET1870084>.
- [13] Verda V, Colella F. Primary energy savings through thermal storage in district heating networks. *Energy* 2011;36(7):4278–86.
- [14] Fragaki A, Andersen AN, Toke D. Exploration of economical sizing of gas engine and thermal store for combined heat and power plants in the UK. *Energy* 2008;33(11):1659–70.
- [15] Johara DK, Sharmab D, Soni SL. Comparative studies on microcogeneration, microcogeneration with thermal energy storage and microtrigeneration with thermal energy storage system using same power plant. *Energy Convers Manag* 2020;220.
- [16] Pérez-Iribarren E, González-Pino I, Azkor Z. Optimal design and operation of thermal energy storage systems in micro-cogeneration plants. *Appl Energy* 2020; 265(1).
- [17] Mongibello L, Capezzuto M, Graditi G. Technical and cost analyses of two different heat storage systems for residential micro-CHP plants. *Appl Therm Eng* 2014;71(2): 636–42.
- [18] Sarbu I, Sebarchievici C. A comprehensive review of thermal energy storage. *Sustainability Journal* 2018;10(191).
- [19] Xu H, Szea JY, Romagnoli A, Py X. Selection of phase change material for thermal energy storage in solar air conditioning systems. In: The 8th international conference on applied energy – icae2016; 2017. Singapore.
- [20] Fazilati MA, Alemrajabi AA. Phase change material for enhancing solar water heater, an experimental approach. *Energy Convers Manag* 2013;73:138–45.
- [21] Cabeza LF, Ibanez M, Sole' C, Rocaa J, Nogue's M. Experimentation with a water tank including a PCM module. *Sol Energy Mater Sol Cells* 2006;90:1273–82.
- [22] Pielichowska K, Pielichowski K. Phase change materials for thermal energy storage. *Progress in Material Science* 2014;(65):67–123.
- [23] T. C. I. o. B. S. E. (CIBSE). Heating - CIBSE guide B1. 2016. Retrieved from, <https://app.knovel.com/hotlink/toc/id:kpHCIBSEG3/heating-cibse-guide-b1/heatin-g-cibse-guide-b1>.
- [24] Groulx D. Design of latent heat energy storage systems using phase change materials. In: *Advances in thermal energy storage systems methods and applications*. United States: Elsevier Science Publishing Co Inc; 2020. p. 331–56.
- [25] Cabeza LF. *Advances in thermal energy storage systems - methods and applications*. Elsevier Science & Technology; 2014.
- [26] Huang L, Noeres P, Petermann M, Doetsch C. Experimental study on heat capacity of paraffin/water phase change emulsion. *Energy Convers Manag* 2010;51(6).
- [27] Climator. ClimSel C58 product specification sheet [Online]. Available: https://www.climator.com/images/pdf/prodblad_climsel_c58_4.1.pdf. [Accessed 5 August 2023].
- [28] Rubitherm. Rubitherm-RT70HC data sheet [Online]. Available: https://www.rubitherm.eu/media/products/datasheets/Techdata_-RT70HC_EN_06082018.PDF. [Accessed 5 August 2023].
- [29] Rubitherm. Rubitherm-RT90HC data sheet [Online]. Available: https://www.rubitherm.eu/media/products/datasheets/Techdata_-RT90HC-in-development_EN_06082018.PDF. [Accessed 5 August 2023].
- [30] PulseICE. PCM products [Online]. Available: <https://www.pcmproducts.net/files/PlusICE%20Range%202021-1.pdf>. [Accessed 5 August 2023].